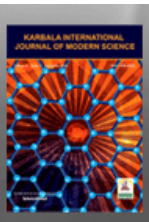

Karbala International Journal of Modern Science

Volume 11 | Issue 3 Article 17

Computational and In vitro Investigation of P. crocatum Bioactive Compounds as Pancreatic Lipase Inhibitors

Gusnia Meilin Gholam
Department of Biochemistry, Faculty of Mathematics and Natural Science, IPB University, Dramaga Campus, Bogor 16680, Indonesia, gusniameilin@apps.ipb.ac.id

Dimas Andrianto
Department of Biochemistry, Faculty of Mathematics and Natural Science, IPB University, Dramaga Campus, Bogor 16680, Indonesia, dimasandrianto@apps.ipb.ac.id

Dewi Anggraini Septaningsih
Advanced Research Laboratory - Institute of Research and Community Service, IPB University, Jalan Palem Raya, Kampus IPB Dramaga, Bogor, 16680, Indonesia, dewi.2986@gmail.com

Mega Safithri
Department of Biochemistry, Faculty of Mathematics and Natural Science, IPB University, Dramaga Campus, Bogor 16680, Indonesia, safithri@apps.ipb.ac.id

Recommended Citation

Gholam, Gusnia Meilin; Andrianto, Dimas; Septaningsih, Dewi Anggraini; and Safithri, Mega (2025) "Computational and In vitro Investigation of P. crocatum Bioactive Compounds as Pancreatic Lipase Inhibitors," *Karbala International Journal of Modern Science*: Vol. 11 : Iss. 3 , Article 17.
Available at: https://doi.org/10.33640/2405-609X.3423

Computational and In vitro Investigation of P. crocatum Bioactive Compounds as Pancreatic Lipase Inhibitors

Abstract

Obesity, a prevalent metabolic disorder characterized by excessive fat accumulation, can severely affect overall health if left untreated. This study investigated the potential of a 70% ethanol extract from *Piper crocatum* (red betel) leaves as an *in vitro* inhibitor of pancreatic lipase (PL), supported by computational analyses to identify alternative compounds to orlistat. The phytochemical profile was characterized using LC-MS/MS, revealing alkaloids and terpenoids with contents of 1.1 ± 0.01 mg CE/g and 3.14 ± 0.3 mg UAE/g, respectively. The extract exhibited 49 ± 9.1% inhibition of PL activity. Molecular docking identified three promising compounds: calanolide A (10.43 kcal/mol), myricanone (10.04 kcal/mol), and (-)-8-prenylnaringenin (9.49 kcal/mol). Based on DFT studies, these compounds showed favorable ADMET and electronic properties. MD simulations demonstrated that the PL-calanolide A complex maintained high conformational stability over 100 ns with a binding energy of 150.75 kJ/mol (MM-PBSA). These findings suggest that red betel leaf extract may serve as a promising natural pancreatic lipase inhibitor, as supported by robust *in vitro* and computational evidence supporting its potential for future anti-obesity drug development.

Keywords

obesity; Computational Studies; density functional theory; Pancreatic lipase

RESEARCH PAPER

Computational and *In vitro* Investigation of *P. crocatum* Bioactive Compounds as Pancreatic Lipase Inhibitors

Gusnia M. Gholam [a], Dimas Andrianto [a,b], Dewi A. Septaningsih [c], Mega Safithri [a,d,*]

[a] Department of Biochemistry, Faculty of Mathematics and Natural Science, IPB University, Dramaga Campus, Bogor, 16680, Indonesia
[b] Halal Science Center, IPB University, 16127, West Java, Indonesia
[c] Advanced Research Laboratory – Institute of Research and Community Service, IPB University, Jalan Palem Raya, Kampus IPB Dramaga, Bogor, 16680, Indonesia
[d] Tropical Biopharmaca Research Center (Biopharmaca), Institute for Research and Community Service, IPB University, Bogor, Indonesia

Abstract

Obesity, a prevalent metabolic disorder characterized by excessive fat accumulation, can severely affect overall health if left untreated. This study investigated the potential of a 70 % ethanol extract from *Piper crocatum* (red betel) leaves as an *in vitro* inhibitor of pancreatic lipase (PL), supported by computational analyses to identify alternative compounds to orlistat. The phytochemical profile was characterized using LC-MS/MS, revealing alkaloids and terpenoids with contents of 1.1 ± 0.01 mg CE/g and 3.14 ± 0.3 mg UAE/g, respectively. The extract exhibited 49 ± 9.1 % inhibition of PL activity. Molecular docking identified three promising compounds: calanolide A (10.43 kcal/mol), myricanone (10.04 kcal/mol), and (−)-8-prenylnaringenin (9.49 kcal/mol). Based on DFT studies, these compounds showed favorable ADMET and electronic properties. MD simulations demonstrated that the PL-calanolide A complex maintained high conformational stability over 100 ns with a binding energy of 150.76 kJ/mol (MM-PBSA). These findings suggest that red betel leaf extract may serve as a promising natural pancreatic lipase inhibitor, as supported by robust *in vitro* and computational evidence supporting its potential for future anti-obesity drug development.

Keywords: Obesity, Computational studies, Density functional theory, Pancreatic lipase

1. Introduction

Obesity, a global metabolic disorder, is characterized by excessive fat accumulation in adipose tissue, leading to numerous health complications, such as cardiovascular diseases, diabetes, and hyperlipidemia. With rising obesity rates worldwide, there is a critical need for effective strategies to manage and treat this condition. A primary target in obesity treatment is the inhibition of pancreatic lipase (PL), an enzyme responsible for the hydrolysis of dietary fats in the gastrointestinal tract. Although pharmacological agents, such as orlistat, have demonstrated efficacy in inhibiting PL, their use is often limited by adverse effects, including gastrointestinal discomfort and allergic reactions. Consequently, there is an increasing demand for safer natural alternatives to treat obesity [1–6].

Medicinal plants have long been utilized in traditional medicine to treat various ailments, and their therapeutic potential continues to be explored in modern pharmacology. In traditional Chinese medicine (TCM), numerous herbs belonging to the

Received 10 February 2025; revised 30 June 2025; accepted 3 July 2025.
Available online 31 July 2025

* Corresponding author at: Department of Biochemistry, Faculty of Mathematics and Natural Science, IPB University, Dramaga Campus, Bogor, 16680, Indonesia.
E-mail address: safithri@apps.ipb.ac.id (M. Safithri).

https://doi.org/10.33640/2405-609X.3423

Piperaceae family have been utilized for centuries. *Piper crocatum*, a species of the Piper genus, a species within the Piper genus, is well recognized for its medicinal properties and has been traditionally used to manage various health conditions such as asthma and rheumatism. Despite the broad use of the Piper species, the potential of *P. crocatum* in treating obesity remains underexplored, making it a compelling candidate for further investigation [7–12].

Flavonoids and polyphenolic compounds, which are abundant in medicinal plants, are known for their diverse pharmacological effects, including antioxidant, anti-inflammatory, and anti-obesity activities. Recent studies have demonstrated the potential of these compounds to modulate metabolic pathways, particularly those involved in fat digestion and absorption. Harnessing these bioactive molecules for therapeutic applications may provide safer alternatives to conventional anti-obesity drugs, such as orlistat [8,13].

In drug discovery, *in silico* approaches have emerged as powerful tools for identifying and screening potential drug candidates. These computational techniques can predict key properties, such as binding affinity, toxicity, and bioavailability of drug candidates, significantly accelerating the drug discovery process. Molecular docking and molecular dynamics (MD) simulations have proven to be effective in predicting the interactions between drug candidates and their target proteins, offering valuable insights into their potential efficacy and safety. These methods have been successfully applied in the development of drugs for various diseases, including cancer and metabolic disorders [14–16].

This study aimed to evaluate the anti-obesity potential of *P. crocatum* through a combination of *in vitro* enzyme assays and computational docking studies. We hypothesized that bioactive compounds in *P. crocatum* can effectively inhibit pancreatic lipase activity and reduce fat absorption, thus serving as natural alternatives to orlistat. Using a 70 % ethanol extract of *P. crocatum* leaves, we assessed its inhibitory effects against PL and identified key active compounds via molecular docking. Furthermore, *in silico* analyses were conducted to predict the pharmacokinetic properties and binding affinities of these compounds, providing additional support for their potential as anti-obesity agents. This study contributes to the ongoing search for novel, safe, and plant-derived treatments for obesity and its associated metabolic disorders.

2. Materials and methods

2.1. Plant material, chemicals and reagents

This study employed Red betel (*Piper crocatum*) leaves were collected from Solo, Central Java, Indonesia. The samples were acquired from the Tropical Biopharmaca Research Center, IPB University, Bogor, Indonesia, under sample collection number BMK0531112023. Phytochemical analysis utilized various reagents, including phosphate buffer (pH 4.7), bromocresol green, chloroform, caffeine, perchloric acid, and a vanillin/glacial acetic acid (5 % w/v) solution. Additional chemicals included glacial acetic acid and ursolic acid. For the *in vitro* assays, 70 % ethanol was used along with pancreatic lipase (PL, Otto Chemie, code L 1471, CAS 9001-62-1), *p*-Nitrophenol (Otto Chemie, code N 1887), and *p*-Nitrophenyl butyrate (Otto Chemie, code N 8789). The *in silico* analysis employed the PL enzyme with Protein Data Bank (PDB) code 1LPB.

2.2. Preparation of the extract

The collected red betel (*Piper crocatum*) leaves were thoroughly washed under running water and drained. The leaves were then chopped into smaller pieces and dried in an oven at 50 °C for three days. Once dried, the leaves were blended and sieved to produce simplicia with an 80-mesh size, which were stored in plastic containers at room temperature until further use. Extraction was conducted using the maceration method. Specifically, 25 g of the prepared simplicia was soaked in 100 mL of 70 % ethanol at a ratio of 1:4 and agitated at 130 rpm in a water bath shaker at room temperature for 24 h. The mixture was then filtered to separate the liquid extract from the plant residues. The filtrate was concentrated using a rotary evaporator (Eyela 1110S-WD) at 50 °C to obtain a crude extract. This procedure was repeated three times to maximize the yield of bioactive compounds [17].

2.3. Determination of total alkaloids content

Two milliliters of the extract solution with a concentration of 1000 ppm was mixed with 2 mL of phosphate buffer (pH 4.7), 2 mL of Bromocresol Green (BCG), and 3 mL of chloroform. The mixture was then extracted with 1 mL of chloroform using a vortex, with the vortexing repeated three times. One milliliter of chloroform was added for each vortex repetition. The resulting extract was evaporated using a water bath for 15 min. Finally, 10 mL of

chloroform was added, and the absorbance was measured at 273 nm. Caffeine was used to create the standard calibration curve [18].

2.4. Determination of total terpenoid content

Total terpenoids were quantified following the method described by Biswas et al. [19], with ursolic acid as the standard. Two hundred microliters (200 μL) of the 70 % ethanol extract of red betel leaves from Solo at a concentration of 1000 ppm were mixed with 1 mL of perchloric acid. Subsequently, 300 μL of vanillin/glacial acetic acid (5 % w/v) solution was added, followed by 0.5 mL of glacial acetic acid. The mixture was incubated in the dark at room temperature for 2 h. After incubation, 200 μL of the mixture was transferred to a 96-well flat-bottom microplate, and absorbance was measured at 535 nm [19].

2.5. Phytochemical analysis with LC-MS/MS

Phytochemical profiling was conducted following the methodology described by Purnama [20] to identify secondary metabolites using LC-MS/MS. The analysis was performed using a Thermo Scientific Vanquish Flex UHPLC coupled with a Q Exactive Plus Orbitrap HRMS. The mobile phase consisted of 0.1 % formic acid in water and 0.1 % acetonitrile in water, and compound separation was achieved using an Accucore™ Phenyl Hexyl column. Data were processed using Compound Discoverer 3.2 software, which facilitated retention time alignment, detecting unknown compounds, and normalizing data.

2.6. In vitro *lipase inhibition assay*

Pancreatic lipase (PL) activity was evaluated following a modified protocol based on Jo et al. [21], with modifications. Orlistat was used as the positive control. A 10 mM p-nitrophenol solution was used to generate a standard curve. An enzyme solution of 0.1 mg/mL was prepared by dissolving PL in 0.1 M Tris-HCl buffer at pH 7.6. Similarly, a 10 mM solution of p-nitrophenyl butyrate (p-NPB) was prepared. The assay mixture consisted of 180 μL of PL solution, 10 μL of p-NPB, and 10 μL of 70 % ethanol extract of red betel leaves, incubated for 55 min. Absorbance was measured at 427 nm using a microplate reader. Enzyme activity was measured as the percentage inhibition (%).

2.7. Enzyme selection and structural preparation

The pancreatic lipase enzyme structure (PDB ID: 1LPB) was prepared using the YASARA Structure software with appropriate parameter adjustments. The preparation steps included the removal of water molecules, addition of hydrogen atoms, application of the AMBER14 force field, and energy minimization. Unnecessary molecules were discarded while retaining chains A and B. The enzyme was modeled at pH 7.4 and saved in PDB format for subsequent analyses [22].

2.8. Ligand structural preparation

Candidate compounds identified by LC-MS/MS were subjected to *in silico* evaluation. We prepared the compounds (ligands) by obtaining their structures from PubChem and storing them in the SMILES format. The structures were downloaded from (. sdf) format and prepared by adding hydrogen atoms, using NOVA, and performing energy minimization with the YASARA structure. All prepared ligands were then saved in (*ligands.sdf) format [22].

2.9. Assessment of the binding pocket of lipase pancreatic

The binding site of the PL enzyme (1LPB) was predicted using the CavityPlus web server (Version 2022 09) (pkumdl.cn:8000/cavityplus/index. php#/). The enzyme prepared in a previous study (. pdb) format containing chains A and B was uploaded to the CavityPlus server and configured in no-ligand mode. The other parameters were set to default. The outcomes were collected in WinRAR format for further analysis. Additionally, the results are accessible on the CavityPlus server [23].

2.10. Molecular docking

Molecular docking simulations were performed using the VINA method implemented in the YASARA Structure through the dock_runscreening file. In this algorithm file, docking simulations were run for 25 sets of each ligand, with the best poses saved as 1. During the simulation, the compounds were sorted based on their binding energies. Molecular docking utilized the AMBER14 force field, where the enzyme remained rigid, while the ligands were flexible. The docking area was set in a cube with dimensions X-size 87.63 Å, Y-size 87.63 Å, and Z-size 87.63 Å for molecular docking [24]. Subsequently, interaction analysis was conducted using BIOVIA Discovery Studio software.

2.11. ADMET and DFT studies

Compounds exhibiting the highest binding affinities were subjected to ADMET profiling using the

SwissADME server (http://www.swissadme.ch/). The collected SMILES were uploaded to this server, and the results were used to identify the ADMET properties of the selected compounds. Density functional theory (DFT) with the B3LYP/3–21G functional set was used to calculate the HOMO energy, LUMO energy, and energy gap of the selected compounds. The computations were performed using the Gaussian 09 W software package [25,26].

2.12. Molecular dynamics (MD) simulation

MD simulation settings were configured in the md_run.mcr macro. The simulation was run at a water density of 0.997 g mL^{-1} with 0.9 % NaCl at pH 7.4. A temperature of 310 K was used to control the enzyme-ligand complex environment during the MD simulation. This study employed a trajectory of 100 ns and utilized the AMBER14 force field, cutoff of 8, and periodic boundary conditions. After the 100 ns trajectory was completed, post-MD analysis was carried out by executing the md_analyze.mcr and md_analyzeres.mcr macros. The analysis considered several parameters to assess the stability of the enzyme-ligand complex, such as RMSD, RMSF, radius of gyration (Rg), solvent-accessible surface area (SASA), and H-bond [27].

2.13. Calculation of binding energy using MM-PBSA

Binding free energy of enzyme-ligand complexes was calculated using the MM-PBSA method implemented in the md_analyzebindenergy.mcr macro, providing quantitative assessment of interaction strength [28].

3. Results

3.1. Total alkaloid content

The 70 % ethanol extract of red betel leaves from Solo was subjected to quantitative analysis to determine the amount of alkaloids contained in the extract. The total alkaloid content was calculated using the caffeine standard curve equation $y = 0.0115x + 0.1002$, which yielded an R^2 value of 0.9912. The total alkaloid content in the 70 % ethanol extract of red betel leaf from Solo sample was found to be 1.1 ± 0.014 mg CE/g dry weight. The results of the total alkaloid measurements are presented in Fig. 1A.

3.2. Total terpenoid content

The total terpenoid content was calculated using the standard curve equation for ursolic acid, $y = 0.0008x + 0.0876$, which resulted in an R^2 value of 0.9715. Total terpenoids were calculated as milligrams of ursolic acid equivalents per gram of dried plant extract (mg UAE/g). Therefore, the total terpenoid measurement results indicate that the 70 % ethanol extract of red betel leaf from Solo sample contains 3.14 ± 0.3 mgUAE/g of terpenoids. The results are shown in Fig. 1B.

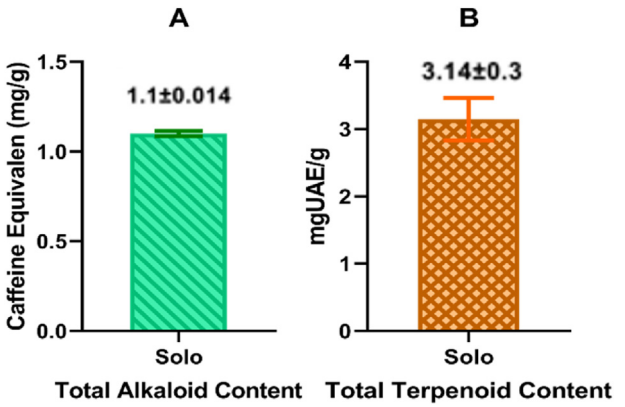

Fig. 1. Measurement of total alkaloids and terpenoids in 70 % ethanol extract of red betel leaf from Solo. A) Total alkaloids in 70 % ethanol extract of red betel leaf from Solo. B) Total terpenoids in 70 % ethanol extract of red betel leaves from Solo.

3.3. Phytochemical analysis with LC-MS/MS

Based on the LC-MS/MS results, several compounds were successfully identified from the 70 % ethanol extract of red betel leaf, as shown in Table 1. From the identification results, various compounds from different classes were observed, including alkaloids, flavonoids, tannins, steroids, lignans, benzene, and coumarins. LC-MS/MS is particularly suitable for detecting non-volatile and thermally labile compounds; thus, molecular weight data were used to facilitate the identification of high-molecular-weight, non-volatile constituents.

3.4. In vitro *pancreatic lipase enzyme activity*

This study investigated the effects of 70 % ethanol extract of red betel leaf against pancreatic lipase compared to the positive control orlistat. Initially, orlistat was tested against the enzyme to assess its effect on enzyme activity. The results showed an enzyme activity of 80.4 U. In contrast, the addition of the 70 % ethanol extract of red betel leaf from Solo at a concentration of 1000 ppm in the sample-enzyme testing showed an enzyme activity of 145.6 U. The enzyme activity levels are presented in Fig. 2A. These results correlated with the percentage inhibition calculation. As observed in Fig. 2B, orlistat exhibited an inhibition of 71.8 ± 6.3 %, while the

Table 1. Identification of compounds in the 70 % ethanol extract of red betel leaf from Solo was performed using LC-MS/MS.

Retention time (min)	Compounds	Molecular weight	Molecular Formula
16.9	TU4153400	460,2082	C25 H32 O8
14.1	Delta-corlin	400,1875	C23 H28 O6
16.9	2-(4-Allyl-2,6-dimethoxyphenoxy)-1-(3,4,5-trimethoxyphenyl)-1-propanol	418,1978	C23 H30 O7
18.08	Xanthohumol	354,1456	C21 H22 O5
15.4	Cyclandelate	276,1715	C17 H24 O3
16.3	Piperine	285,1357	C17 H19 N O3
16.8	calanolide A	370,17659	C22 H26 O5
16.9	4,4-Bis[4-(acetyloxy)phenyl]3-hexanone	368,16133	C22 H24 O5
18.9	Shogaol	276,17146	C17 H24 O3
18.01	Schisandrin C	384,1561	C22 H24 O6
18.07	Fusarin C	431,1927	C23 H29 N O7
18.3	Mycophenolate mofetil	433,2086	C23 H31 N O7
15.3	myricanone	356,16124	C21 H24 O5
26.6	Pheophorbide A	592,267	C35 H36 N4 O5
17.6	(−)-8-Prenylnaringenin	340,1302	C20 H20 O5

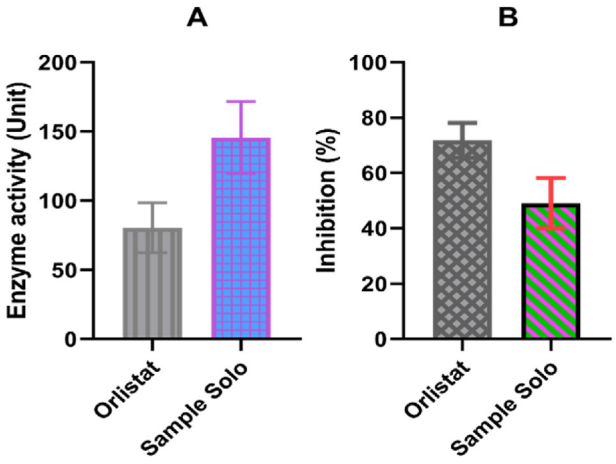

Fig. 2. Enzyme activity and percentage inhibition of pancreatic lipase by 70 % ethanol extract of red betel leaves from Solo. Orlistat served as the positive control. A) Enzymatic activity. B) Percentage of inhibition.

Solo sample showed an inhibition of 49 ± 9.1 %. At a low concentration of 100 ppm, orlistat was able to inhibit much more strongly than the red betel extract at 1000 ppm. These results imply that orlistat is a pure compound, whereas the red betel extract contains various phytochemicals, leading us to predict diverse activities during the inhibition process. To explore this further, computational analysis is being pursued to identify individual phytoconstituents with superior lipase-inhibitory mechanisms compared with orlistat.

3.5. Binding pocket analysis

Research on identifying the active site of the pancreatic lipase enzyme is crucial to predict amino acid residues that may bind to drug candidates, thereby predicting the drug's ability to react with the pancreatic lipase enzyme target. The results revealed a strong druggability area, with a drug-score value of 1696. The results are presented in Table 2. The volume of 695.88 Å3 and surface area of 468.75 Å2 predicted 41 amino acid residues detected within this enzyme.

3.6. Post-docking analysis

The results showed that many compounds had more binding energy than the control drug (Table 3). This study focused on the three best ones, namely calanolide A (10.43 kcal/mol), myricanone (10 kcal/mol), and (−)-8-Prenylnaringenin (9.49 kcal/mol).

We analyzed the drug-control complex and the three best complexes. Fig. 3A shows that the orlistat complex interacts with the catalytic triad Ser152 and His263 through hydrogen bonds. The amino acid residues and types of interactions present in the orlistat complex were also observed in the calanolide A complex (Fig. 3B).

In the PL-orlistat enzyme complex, orlistat interacts with the target lipase through the amino acid residues Tyr114, Asp79, Gly78, Phe77, Trp252, and Arg256. Calanolide A forms hydrogen bonds with His263, Ser152, and Gly76, whereas hydrophobic interactions occur with Leu264, Arg256, Ala260, Ile78, Ala259, Phe215, Tyr114, Ile209, Pro180, and Ala178. In the PL-myricanone enzyme complex, it was observed that the ligand interacts with His263, Phe77, Ser152, Tyr114, Ala128, Pro180, and Phe215.

In the PL-(−)-8-Prenylnaringenin enzyme complex, the ligand interacts with the amino acid residues Ile78, His263, Ser157, Phe77, Leu153, Pro180, Phe215, Ala260, and Ala1259. These findings

Table 2. Prediction of the Active Site of PL Enzyme PDB ID 1LPB using CavityPlus

Cavity No.	Predicted Maximal pKd	Predicted Average pKd	DrugScore	Druggability	Surface Area (Å^2)	Volume (Å^3)	Residues
1.	10.61	6.95	1696.00	Strong	468.75	695.88	Leu213, Ala178, Phe215, Trp252, Gly214, Ala259, Ala260, Lys80, Asp257, Leu264, His263, Gly76, Glu179, Arg111, Thr255, Asp176, Ser118,Val210, His75, Glu83, Phe258, Gly154, His151, Ile209, Phe77, Trp85, Pro177, Leu153, Asp79, Tyr114, Gly216, Arg256, Ile251, Tyr267, Ile78, Cys261, Asp205, Ser152, Cys181, Thr115, Pro180

Table 3. Molecular docking of compounds from 70 % ethanol extract of red betel leaf from Solo against the PL enzyme.

CID	Compound	Binding energy (kcal/mol)
64972	Calanolide A	10.43
161748	Myricanone	10.0
480764	(−)-8-prenylnaringenin	9.49
91438	D-Corlin	9.42
253193	Pheophorbide A	9.35
6435894	Fusarin C	9.18
571099	Tu4153400	9.04
639665	Xanthohumol	8.19
638024	Piperine	8.14
2893	Cyclandelate	8
5281078	Mycophenolate mofetil	7.85
10477119	2-(4-Allyl-2,6-dimethoxyphenoxy)-1-(3,4,5-trimethoxyphenyl)-1-propanol	7.25
119112	Schisandrin C	7.23
240071	4,4-Bis[4-(acetyloxy)phenyl]3-hexanone	6.89
3034010	Orlistat (**Control drug**)	6.87
5281794	Shogaol	6.76

demonstrate that the selected ligands interacted effectively through both hydrogen bonding and hydrophobic interactions.

Fig. 3C illustrates that the myricanone compound interacts with the oxyanion hole Phe77 and the catalytic triad Ser152 through hydrogen bonds, whereas the catalytic triad His263 forms a Pi-cation interaction with the aromatic ring of myricanone. In the complex, hydrogen bonds occur due to the hydroxyl group (OH). (−)-8-Prenylnaringenin forms hydrogen bonds with the catalytic triad Ser152 and oxyanion hole Phe77 (Fig. 3D). Additionally, hydrophobic interactions were present within the complex. Interestingly, in the calanolide A complex, hydrophobic interactions were more dominant compared to orlistat and the other two compounds analyzed.

3.7. ADMET and DFT analysis

We analyzed potential drug candidates to assess their similarity to safe human drugs through structural molecular analysis or physicochemical analysis. We calculated ADMET properties for calanolide A, myricanone, and -(−)-8-Prenylnaringenin as presented in Supplementary Material 1 (https://kijoms.uokerbala.edu.iq/cgi/editor.cgi?article=3423&window=additional_files&context=home). Based on the predictions, the results showed good TPSA values for all three compounds, correlating with high GI absorption values. The consensus log Po/w values for all three compounds indicated optimal physicochemical and ADME properties when used as oral drugs for humans. This also correlates with a “yes” category in the Lipinski rule, indicating no violations of Lipinski's rule. Toxicity properties were also predicted to be safe when analyzed based on the AMES toxicity and hepatotoxicity. However, we observed that the BBB permeability prediction was only for calanolide A and myricanone.

The B3LYP/3−21G basis set within the computational algorithm of the Gaussian 09 software was utilized to compute the HOMO and LUMO energies. These energies form the FMOs. Fig. 4 displays the three selected compounds, each highlighted in red for the positive phase and in green for the negative phase. In this context, the stability of the selected compounds was assessed by examining the energy gap. A larger energy gap indicates greater stability and lower reactivity. These results indicate that the compound with the lowest energy gap (0.15 eV) is calanolide A.

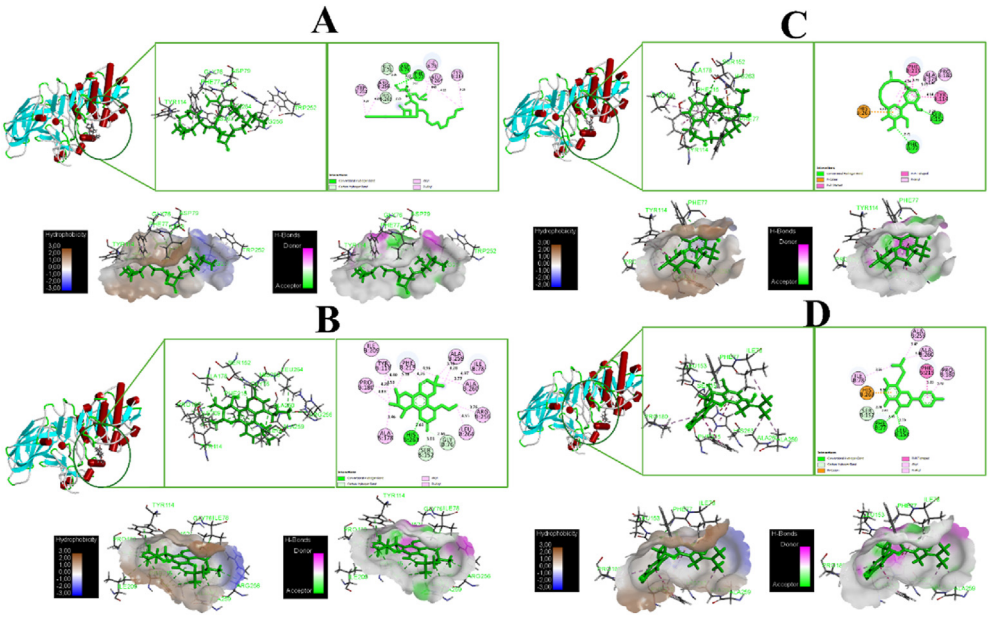

Fig. 3. Visualizing the 2D and 3D enzyme-ligand complexes using BIOVIA Discovery Studio. The visualization displays the interactions within the complex and the hydrophobicity and H-bond areas in each complex. A) 1LPB-orlistat complex B) 1LPB-calanolide A complex C) 1LPB-myricanone complex D) 1LPB-(−)-8-Prenylnaringenin complex.

3.8. Post-MD analysis

MD simulations were conducted at 310 K using the AMBER14 force field to analyze the stability of the selected enzyme-ligand complexes over a 100 ns trajectory using the YASARA structure. We analyzed RMSF, which helped us understand the fluctuations at the amino acid residue level, impacting stability within the enzyme-ligand complex. The RMSF graph produced over the 100 ns trajectory, as visualized in Fig. 5, shows fluctuations in several amino acid residues. However, the average RMSF values for each complex were as follows: PL-orlistat 1.51 Å, PL-calanolide A 1.42 Å, PL-myricanone 1.45 Å, and PL-(−)-8-Prenylnaringenin 1.63 Å. Therefore, the PL-calanolide A complex had the best stability at the amino acid residue level.

RMSDCa analysis indicated the stability of the enzyme-ligand complex conformations. The results

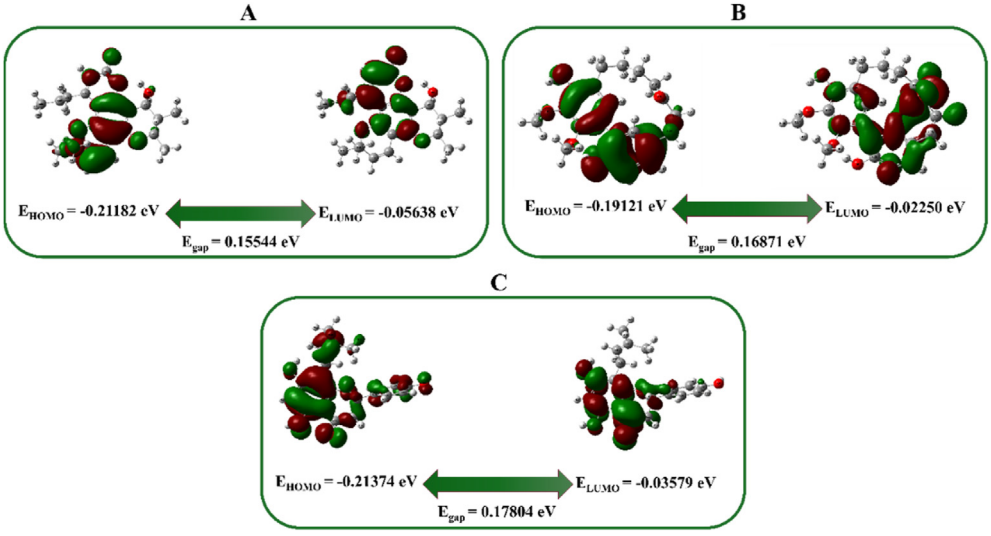

Fig. 4. Visualizations and values of HOMO, LUMO, and energy gap. A) PL-calanolide A complex B) PL-myricanone complex C) PL-(−)-8-Prenylnaringenin complex.

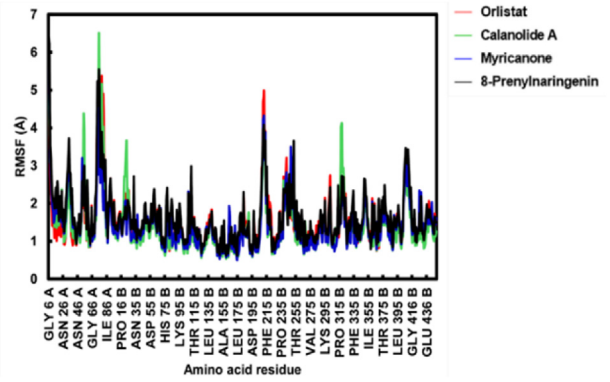

Fig. 5. Production of RMSF graphs by the four complexes over a 100 ns trajectory in the simulated MD.

show that the highest RMSDCa value in the produced graph, as shown in Fig. 6A, is in the PL-orlistat complex at 3.94 Å. Conversely, the lowest value is in the PL-calanolide A complex at 2.89 Å. The average RMSDCa graph production values are lowest in the PL-calanolide A complex, with an average of 1.95 Å, while the other three complexes exhibit average values exceeding 2 Å.

Rg measurement indicates the stability and tightness of an enzyme-ligand complex. The graph results in Fig. 6B suggest similarities in the values and characteristics among the four complexes. This similarity arises from the fact that all four complexes have average Rg values, in ascending order, of 27.07 Å (orlistat), 27.16 Å (calanolide A), 27.17 Å (myricanone), and 27.19 Å ((−)-8-Prenylnaringenin). They all have average values of approximately 27 Å.

SASA measurement indicates changes in volume and surface properties of the PL enzyme complex. Observing the graph results in Fig. 6C, all four complexes exhibited a similar trend in characteristics. During the 100 ns trajectory, the lowest value was observed in the PL-calanolide A complex at the beginning of the simulation. By the end of the simulation, calanolide A showed an average value of 23195.73 Å against the PL enzyme. Notably, myricanone surprisingly presents the lowest average SASA value in this simulation at 22857.95 Å. This suggests that myricanone has a minimal effect on the surface of the PL enzyme, followed by calanolide A, which also has a minimal effect.

Presence of hydrogen bonds in a complex affects its stability. We observed that PL-orlistat produced a high number of hydrogen bonds, followed by calanolide A, which also exhibited a high number of hydrogen bonds. The results in Fig. 6D show this trend. We indicate that these two complexes are the most stable compared to the others.

This study calculated the binding energy using MM-PBSA calculations, where a more positive value indicated a stronger preference for ligand binding to the PL enzyme. The results showed that orlistat had the highest average binding energy (194.81 kJ/mol), followed by calanolide A (150.75 kJ/mol). Consequently, calanolide A exhibited binding affinities to pancreatic lipase that were most similar

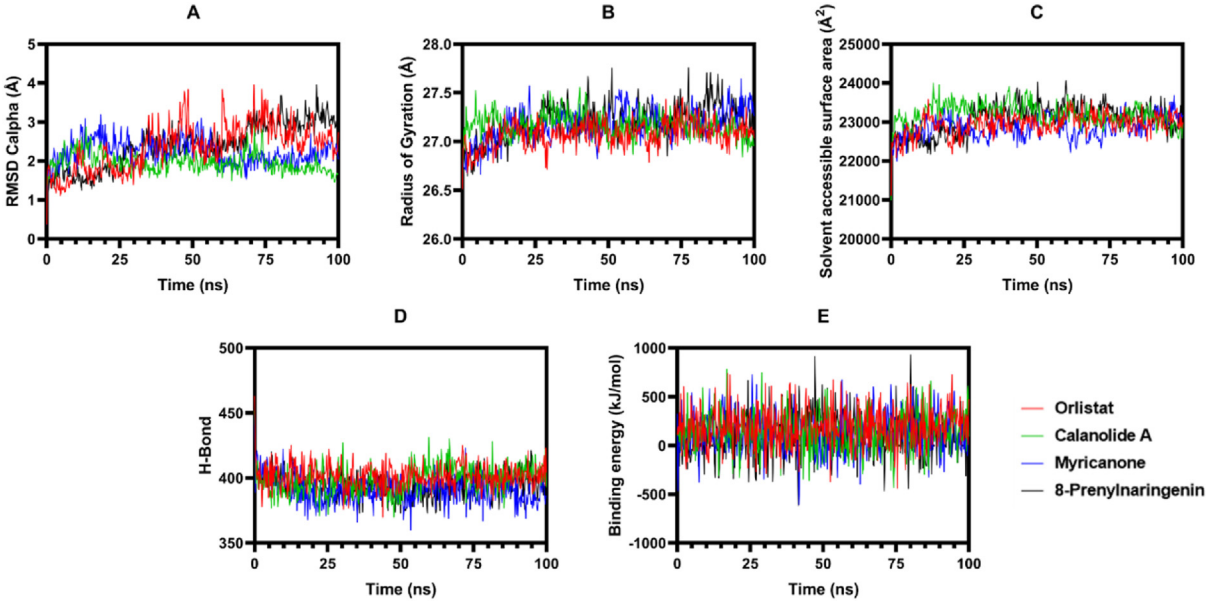

Fig. 6. Production of graphs during the 100 ns MD trajectory simulated against the four complexes. The graph displays several parameters to help analyze the 100 ns trajectory. A) RMSDCalpha B) Radius of gyration C) solvent accessible surface area D) H-bond E) binding energy.

to those observed for orlistat among the ligands evaluated (Fig. 6E).

4. Discussion

To date, no studies have been conducted on red betel leaves (*Piper crocatum*) using both *in vitro* and *in silico* methods. Safithri et al. [29] conducted an *in silico* study analyzing the potential of *Piper crocatum* leaves as pancreatic lipase (PL) inhibitors. Their computational predictions indicated that certain compounds derived from *P. crocatum* exhibit strong binding affinities, suggesting possible inhibitory effects against PL enzymes. In contrast, Prieto-Ridríguez et al. [30] evaluated the lipase inhibitory activity of red betel leaves using both *in vitro* and *in silico* approaches; however, their study focused on *Piper cumanense*, a species distinct from that used in our research. Their investigation, which was the first to assess *P. cumanense* for antidiabetic and anti-obesity applications, identified seven compounds exhibiting catalytic inhibition of PL with IC_{50} values ranging from 28.32 to 55.8 μM. *In vivo* studies have been conducted using red betel leaf extract from *P. betle*, and the results have shown that administering *P. betle* extract at a dose of 500 mg/kg can enhance body oxidation processes without causing side effects or excessive appetite [3].

Red betel leaf samples (*Piper crocatum*) were extracted by maceration using 70 % ethanol as the solvent. 70 % ethanol is also utilized for red betel leaf extraction. For example, Ghani et al. [3] conducted *in vivo* experiments using rats to determine its effects as an obesity preventive measure by inducing 70 % ethanol extract of red betel lef P. betle for 4 weeks. However, it is noteworthy that they did not target PL enzymes. In a different scenario, where the use of ethanol extract for tyrosinase enzyme inhibition testing showed ethanol superiority over n-hexane, Irsal et al. [31].

Our phytochemical profiling via LC-MS/MS revealed compounds consistent with previous reports, including alkaloids, tannins, phenols, and flavonoids. Quantitative analysis of alkaloids and terpenoids aligned with the LC-MS/MS results, confirming the presence of these compound classes in the 70 % ethanol extract of *P. crocatum*.

In Indonesia, which is rich in biodiversity, terpenoids, along with other natural compounds such as saponins, phenolics, alkaloids, lipids, and lectins, are recognized for their immunostimulatory activity. This highlights the importance of quantifying terpenoids as a part of evaluating the overall medicinal value of the plant, including its antibacterial, anti-inflammatory, and antioxidant properties. In this study, we present findings where *Piper crocatum* has been confirmed to contain terpenoids, supporting its potential therapeutic properties. The presence of terpenoids in *P. crocatum* further emphasizes the importance of determining the total terpenoid content, as these compounds may contribute to its medicinal effects, particularly in the context of anti-obesity and immune-modulating activities [32]. Research has focused on the ability of PL enzyme inhibition to reduce obesity as it decreases total body cholesterol. Orlistat is widely used for obesity prevention; however, its side effects, such as abdominal pain, bloating, diarrhea, and oily spotting, necessitate alternative treatments. Medicinal plants offer potential benefits [33]. In this study, a 70 % ethanol extract of *P. crocatum* was tested, and it showed inhibitory activity against PL. We suggest that *P. crocatum* is a potential new anti-obesity agent. *In silico* testing identified single compounds in the extract that could serve as candidate drugs based on their molecular structures.

The combination of *in silico* docking and MD simulation effectively identifies potential drug candidates by studying binding interactions and conformational changes in enzyme-ligand complexes [34]. This approach enhanced the validity of our *in silico* tests and provided a comprehensive analysis of our *in vitro* lipase assays.

From our findings, we observed interactions within the active site (as per the CavityPlus results), indicating that the predicted ligand candidates are likely to interact and effectively inhibit the PL enzyme. The three selected compounds, calanolide A, myricanone, and (−)-8-Prenylnaringenin, bind to oxyanion holes and the catalytic triad in the PL enzyme. Thus, the detection of amino acid residues by CavityPlus confirms previous research showing that certain amino acid residues play crucial roles in lipase enzyme activity. Notably when a ligand interacts with these residues, it is strongly predicted to inhibit PL enzyme activity [33].

We predicted that hydrogen bonding provides stronger binding strength than hydrophobic interactions. This is because hydrogen bonds can enhance the stability of enzyme-ligand complexes [35]. However, it is important to note that we observed hydrophobic interactions in this study that contribute to good stability. A notable example is the PL−calanolide A complex, in which hydrophobic interactions predominate over hydrogen bonding, yet yield the strongest binding affinity observed in our study. These findings are consistent with previous research [35], indicating that hydrophobic regions effectively play a critical role in facilitating effective ligand−receptor binding.

The structural stability and dynamics of the selected compounds with the PL enzyme were evaluated using MD simulations. We observed that all three selected compounds were stable complexes throughout the 100 ns trajectory. Furthermore, our findings confirmed that calanolide A demonstrated the highest structural stability among the compounds identified in the 70 % ethanol extract of *Piper crocatum* (red betel leaves).

Ipek et al. [36] explain the theory of HOMO and LUMO, indicating that the transition of electrons from HOMO to LUMO is understood as electronic absorption. The energy gap calculated in this study is important because it defines the electrical transport properties of a molecule. In other studies, the energy gap has been evaluated as a value that characterizes the chemical reactivity and kinetic stability of molecules [37,38]. The energy gap produced by calanolide A was the lowest, indicating the potential bioactive properties of the molecule. Calanolide A demonstrates a tolerable safety level and has a good pharmacokinetic profile in healthy and HIV-negative individuals. In 2010, it was noted to have entered clinical trials [36].

5. Conclusion

This study highlights the pharmacological efficacy of 70 % ethanol extract of *Piper crocatum* (red betel) leaves, demonstrating significant inhibition (49 ± 9.1 %) of pancreatic lipase (PL), a key enzyme in fat digestion. Phytochemical profiling using LC-MS/MS identified a range of bioactive compounds in the extract, including calanolide A, myricanone, and (−)-8-prenylnaringenin, which exhibited the highest binding affinities in molecular docking studies. Further analysis through molecular dynamics (MD) simulations revealed that these compounds maintained structural stability over a 100 ns trajectory, with calanolide A showing the highest binding energy of 150.76 kJ/mol, as confirmed by the MM-PBSA method. Additionally, all three compounds exhibited favorable ADMET profiles, indicating their potential as drug candidates for future anti-obesity therapies.

The findings of this study suggest that red betel leaf extract possesses promising inhibitory effects on PL, with calanolide A being a particularly strong candidate for further investigation. Despite these promising *in vitro* and computational results, further *in vivo* studies are essential to fully validate the therapeutic potential and bioavailability of these compounds. The integration of experimental and computational approaches has set the foundation for the development of natural-based therapies targeting obesity and related metabolic disorders.

Ethics information

This study did not involve the use of animal or human subjects.

Funding

The authors would like to thank the Penelitian Terapan Kompetitif Nasional 2023 Program for funding this research by contract number 3881/ IT3.L1/ PT.01.03/P/B/2022.

Conflicts of interest

The authors declare that they have no competing interests.

Acknowledgements

The authors would like to thank the *Penelitian Terapan Kompetitif Nasional* 2023 Program for funding this research by contract number 3881/IT3.L1/ PT.01.03/P/B/2022. Additionally, this study is part of Gusnia Meilin Gholam's thesis and was supported by the 2023 National Applied Research Grant.

References

[1] T.C. Farias, J.P. Abreu, J.P.S. Oliveira, A.F. Macedo, A. Rodríguez-Vega, A.P. Tonin, F.S.N. Cardoso, E.C. Meurer, M.G.B. Koblitz, Bioactive properties of peptide fractions from Brazilian soy protein hydrolysates: *In silico* evaluation and experimental evidence, Food Hydrocol. Health 3 (100112) (2023) 1–11, https://doi.org/10.1016/j.fhfh.2022.100112.

[2] A. Alnuaimi, F. Fisayo Ajayi, M. Hamdi, P. Mudgil, H. Kamal, C. Yuen Gan, S. Maqsood, A comparative analysis of anti-lipidemic potential of soybean (Glycine max) protein hydrolysates obtained from different ripening stages: identification, and molecular interaction mechanisms of novel bioactive peptides, Food Chem. 402 (134192) (2023) 1–14, https://doi.org/10.1016/j.foodchem.2022.134192.

[3] Z.D.F. Abdul Ghani, J.M. Husin, A.H.A. Rashid, K. Shaari, Z. Chik, Biochemical studies of Piper betle L leaf extract on obese treated animal using 1H-NMR-based metabolomic approach of blood serum samples, J. Ethnopharmacol. 194 (12) (2016) 690–697, https://doi.org/10.1016/j.jep.2016.10.022.

[4] D. Choe, H. Jang, H.H. Jung, C.S. Shin, T.V. Johnston, D. Kim, S. Ku, *In vivo* anti-obesity effects of Monascus pigment threonine derivative with enhanced hydrophilicity, J. Funct. Foods 67 (103849) (2020) 1–9, https://doi.org/10.1016/j.jff.2020.103849.

[5] B.S. Drew, A.F. Dixon, J.B. Dixon, Obesity management: update on orlistat, Vasc. Health Risk Manag. 3 (6) (2007) 817–821. https://pmc.ncbi.nlm.nih.gov/articles/PMC2350121/.

[6] Y.J. Tak, S.Y. Lee, Long-term efficacy and safety of anti-obesity treatment: where do we stand? Curr. Obes. Rep. 10 (2021) 14–30, https://doi.org/10.1007/s13679-020-00422-w.

[7] B. Jahromi, I. Pirvulescu, K.D. Candido, N.N. Knezevic, Herbal medicine for pain management: efficacy and drug interactions, Pharmaceutics 13 (2) (2021) 251, https://doi.org/10.3390/pharmaceutics13020251.

[8] L. Rajan, D. Palaniswamy, S.K. Mohankumar, Targeting obesity with plant-derived pancreatic lipase inhibitors: a comprehensive review, Pharmacol. Res. 155 (104681) (2020) 1–34, https://doi.org/10.1016/j.phrs.2020.104681.
[9] B. Salehi, Z.A. Zakaria, R. Gyawali, S.A. Ibrahim, J. Rajkovic, Z.K. Shinwari, T. Khan, J. Sharifi-Rad, A. Ozleyen, E. Turkdonmez, M. Valussi, T.B. Tumer, L. Monzote Fidalgo, M. Martorell, W.N. Setzer, Piper species: a comprehensive review on their phytochemistry, biological activities and applications, Molecules 24 (7) (2019) 1364, https://doi.org/10.3390/molecules24071364.
[10] R. Teschke, D. Larrey, D. Melchart, G. Danan, Traditional Chinese medicine (TCM) and herbal hepatotoxicity: RUCAM and the role of novel diagnostic biomarkers such as MicroRNAs, Medicines 3 (3) (2016) 18, https://doi.org/10.3390/medicines3030018.
[11] Y.J. Chai, Y. Go, H.Q. Zhou, H.X. Li, S.J. Lee, Y.J. Park, W. Widowatib, R. Rizal, Y.H. Kim, S.Y. Yang, W. Li, Unusual bicyclo[3.2.1]Octanoid neolignans from leaves of *Piper crocatum* and their effect on pyruvate dehydrogenase activity, Plants 10 (9) (2021) 1855, https://doi.org/10.3390/plants10091855.
[12] A. Setyawati, M.S.H. Wahyuningsih, D.A.A. Nugrahaningsih, C. Effendy, F. Fneish, G. Fortwengel, *Piper crocatum* Ruiz & Pav. ameliorates wound healing through p53, E-cadherin and SOD1 pathways on wounded hyperglycemia fibroblasts, Saudi J. Biol. Sci. 28 (12) (2021) 7257–7268, https://doi.org/10.1016/j.sjbs.2021.08.039.
[13] A. Intharuksa, S. Kuljarusnont, Y. Sasaki, D. Tungmunnithum, Flavonoids and other polyphenols: bioactive molecules from traditional medicine recipes/medicinal plants and their potential for phytopharmaceutical and medical application, Molecules 29 (23) (2024) 5760, https://doi.org/10.3390/molecules29235760.
[14] M. Ouassaf, S. Belaidi, M. Mogren Al Mogren, S. Chtita, S. Ullah Khan, T. Thet Htar, Combined docking methods and molecular dynamics to identify effective antiviral 2, 5-diaminobenzophenonederivatives against SARS-CoV-2, J. King Saud. Univ. Sci. 33 (2) (2021) 1–10, https://doi.org/10.1016/j.jksus.2021.101352.
[15] H. Alonso, A.A. Bliznyuk, J.E. Gready, Combining docking and molecular dynamic simulations in drug design, Med. Res. Rev. 26 (2006) 531–568, https://doi.org/10.1002/med.20067.
[16] J. Aghajani, P. Farnia, P. Farnia, J. Ghanavi, A.A. Velayati, Molecular dynamic simulations and molecular docking as a potential way for designed new inhibitor drug without resistance, Tanaffos 21 (1) (2022) 1–14. https://pmc.ncbi.nlm.nih.gov/articles/PMC9571241/.
[17] M. Safithri, D. Nur Faridah, F. Ramadani, R. Pratama, Antioxidant activity of ethanol extract and fractions of *Piper crocatum* with Rancimat and cuprac methods, Turk. J. Biochem. 47 (2022) 795–801, https://doi.org/10.1515/tjb-2021-0300.
[18] A. Karim, J. Adnan, Irmawati, Determination of total alkaloid content of purple leaf ethanol extract (*Graptophyllum pictum* L.) by UVVis spectrophotometry method, J. Pharm. Pelamonia. 2 (2) (2022) 42–47.
[19] B. Biswas, M. Golder, Md.A. Abid, K. Mazumder, S.K. Sadhu, Terpenoids enriched ethanol extracts of aerial roots of *Ceriops decandra* (Griff.) and *Ceriops tagal* (Perr.) promote diuresis in mice, Heliyon 7 (7) (2021) e07580, https://doi.org/10.1016/j.heliyon.2021.e07580.
[20] E.W. Purnama, M. Safithri, D. Andrianto, Clusterization of red betel leaves (*Piper crocatum*) from various regions in Indonesia based on secondary metabolite fingerprint analysis and cytotoxicity values, IJAR 2 (2023) 170–182, https://doi.org/10.30997/ijar.v4i2.293.
[21] Y.H. Jo, S.B. Kim, Q. Liu, S.-G. Do, B.Y. Hwang, M.K. Lee, Comparison of pancreatic lipase inhibitory isoflavonoids from unripe and ripe fruits of Cudrania tricuspidata, PLoS One 12 (2017) e0172069, https://doi.org/10.1371/journal.pone.0172069.
[22] H. Land, M.S. Humble, YASARA: a tool to obtain structural guidance in biocatalytic investigations, Methods Mol. Biol. 1685 (2018) 43–67, https://doi.org/10.1007/978-1-4939-7366-8_4.
[23] S. Wang, J. Xie, J. Pei, L. Lai, CavityPlus 2022 update: an integrated platform for comprehensive protein cavity detection and property analyses with user-friendly tools and cavity databases, J. Mol. Biol. 435 (2023) 168141, https://doi.org/10.1016/j.jmb.2023.168141.
[24] E. Krieger, G. Vriend, YASARA View—molecular graphics for all devices—from smartphones to workstations, Bioinformatics 30 (2014) 2981–2982, https://doi.org/10.1093/bioinformatics/btu426.
[25] T. Siswina, M.M. Rustama, D. Sumiarsa, E. Apriyanti, H. Dohi, D. Kurnia, Antifungal constituents of *Piper crocatum* and their activities as ergosterol biosynthesis inhibitors discovered via *in silico* study using ADMET and Drug-Likeness Analysis, Molecules 28 (23) (2023) 7705, https://doi.org/10.3390/molecules28237705.
[26] S. Akhter, O. Concepcion, A.F. de la Torre, A. Ali, A.R. Raza, R. Eman, M. Khalid, M.F. ur Rehman, M.S. Akram, H.M. Ali, Synthesis, spectroscopic characterization, DFT and molecular dynamics of quinoline-based peptoids, Arab. J. Chem. 16 (4) (2023) 104570, https://doi.org/10.1016/j.arabjc.2023.104570.
[27] E. Krieger, G. Vriend, New ways to boost molecular dynamics simulations, J. Comput. Chem. 36 (2015) 996–1007, https://doi.org/10.1002/jcc.23899.
[28] E. Krieger, G. Koraimann, G. Vriend, Increasing the precision of comparative models with YASARA NOVA—a self-parameterizing force field, Proteins: Struct. Funct. Bioinf. 47 (2002) 393–402, https://doi.org/10.1002/prot.10104.
[29] M. Safithri, N. Azizah, M. Bintang, R. Kurniasih, Inhibisi ekstrak daun sirih merah terhadap lipase pankreas sebagai antiobesitas secara *in silico*, Pharmamedica J. 8 (2023) 122–129, https://doi.org/10.47219/ath.v8i2.214.
[30] J.A. Prieto-Rodríguez, K.P. Lévuok-Mena, J.C. Cardozo-Muñoz, J.E. Parra-Amin, F. Lopez-Vallejo, L.E. Cuca-Suárez, O.J. Patiño-Ladino, *In vitro* and *In silico* study of the α-glucosidase and lipase inhibitory activities of chemical constituents from piper cumanense (Piperaceae) and synthetic analogs, Plants 11 (2022) 2188, https://doi.org/10.3390/plants11172188.
[31] R.A.P. Irsal, M. Safithri, D. Andrianto, E. Mardliyati, Flavonoid concentration and tyrosinase inhibition activity of ethanol extract of *Piper crocatum* (*Piper crocatum* var. Ruiz & Pav) from various regions in Indonesia and their correlations, J. Kim. Valensi. 9 (2023) 42–52, https://doi.org/10.15408/jkv.v9i1.31426.
[32] Y. Purnomo, A. Tilaqza, M.S. Zubair, A.Z. Mustopa, Immunopotentiator of terpenoid from *Hibiscus tiliaceus* leaf fraction as candidate of vaccine adjuvants with *in silico* study, S. Afr. J. Bot. 172 (2024) 19–30, https://doi.org/10.1016/j.sajb.2024.06.051.
[33] Y. Vangoori, A. Dakshinamoorthi, S. Kavimani, Prominent pancreatic lipase inhibition and free radical scavenging activity of a *Myristica fragrans* ethanolic extract *in vitro*. Potential role in Obesity Treatment, Maed. - J. Clin. Med. 14 (2019) 254–259, https://doi.org/10.26574/maedica.2019.14.3.254.
[34] S. Mahmud, S. Biswas, G. Kumar Paul, M.A. Mita, S. Afrose, Md. Robiul Hasan, Mst. Sharmin Sultana Shimu, M.A.R. Uddin, Md. Salah Uddin, S. Zaman, K.M. Kaderi Kibria, Md. Arif Khan, T. Bin Emran, Md. Abu Saleh, Antiviral peptides against the main protease of SARS-CoV-2: a molecular docking and dynamics study, Arab. J. Chem. 14 (2021) 103315, https://doi.org/10.1016/j.arabjc.2021.103315.
[35] X. Chen, X. Li, Y. Li, Toxicity inhibition strategy of microplastics to aquatic organisms through molecular docking, molecular dynamics simulation and molecular modification, Ecotoxicol. Environ. Saf. 226 (2021) 112870, https://doi.org/10.1016/j.ecoenv.2021.112870.
[36] C. Ipek, H. Gümüş, M. Şimşek, M. Tosun, DFT and molecular docking study of 1-(2′-Thiophen)-2-propen-1-one-3-(2,3,5-trichlorophenyl) (TTCP) molecule as antiviral to Covid-19 main protease, Arab. J. Sci. Eng. 48 (2023) 1031–1040, https://doi.org/10.1007/s13369-022-07293-4.

[37] U. Holikulov, M. Khodiev, N. Issaoui, A. Jumabaev, N. Kumar, O.M. Al-Dossary, Exploring the non-covalent interactions, vibrational and electronic properties of 2-methyl-4-hydro-1,3,4-triazol-thione-5 in different solutions, J. King Saud. Univ. Sci. 36 (2024) 103164, https://doi.org/10.1016/j.jksus.2024.103164.

[38] N. Lefi, A.S. Kazachenko, M. Raja, N. Issaoui, A.S. Kazachenko, Molecular structure, spectral analysis, molecular docking and physicochemical studies of 3-Bromo-2-hydroxypyridine monomer and dimer as bromodomain inhibitors, Molecules 28 (6) (2023) 2669, https://doi.org/10.3390/molecules28062669.